Transient dynamics of laminated beams: an evaluation with a higher-order refined theory

Sudhakar R. Marur[a], Tarun Kant[b]

[a]CSS Foundation for Research in Finite Elements, B4/4, Vaigai Nagar, Madurai 625 016, India
[b]Department of Civil Engineering, Indian Institute of Technology, Powai, Mumbai 400 076, India

Abstract

A higher-order refined model with seven degrees of freedom per node and cubic axial, quadratic transverse shear and linear transverse normal strain components is presented for the transient dynamic analysis of composite and sandwich beams. This shear correction coefficient free theory considers each layer of the beam to be in a state of plane stress. A special lumping scheme is employed for the evaluation of the diagonal mass matrix and a central difference predictor scheme is used to solve the dynamic equilibrium equation. The excellent performance of the higher-order model in comparison with the first-order theory is clearly brought out through numerical experiments. © 1998 Elsevier Science Ltd. All rights reserved.

1. Introduction

The C^1 finite-element formulation based on Euler–Bernoulli theory has been extensively applied to the linear and non-linear dynamic analysis of beams and frames [1–4]. The first-order shear deformation theory of Timoshenko [5] has been the basis of many anisoparametric beam elements [6–9] till the advent of C^0 beam element by Hughes et al. [10]. Both these types of elements have been used for the transient dynamics of frames for ascertaining their relative performance by Kant and Marur [11].

The limitations of the classical and first-order theory, the development of the second- [12], third- [13] and fourth-order [14] theories along with the need for a refined theory have been discussed in detail in [16].

The higher-order theory of Kant and Gupta [15] considered both the transverse shear and normal strains along with isoparametric elements for the bending and vibration studies of isotropic beams. This theory was then extended to the vibration problem of laminated beams [16]. Subsequently, the dynamic response of sandwich and composite beams was evaluated with higher-order models [17]. However, this study considered only the transverse shear strain component.

As the transverse normal strain effect becomes vital with the depth of the cross-section becoming larger, a higher-order flexural theory with cubic axial, quadratic transverse shear and linear transverse normal strain components is proposed for the transient dynamic analysis of laminated beams. Each layer of the beam is considered to be in a state of plane stress with the constitutive equation derived from the reduction of the 3D stress–strain relationship of an orthotropic lamina.

2. Higher-order model

The higher-order displacement model, based on Taylor's series expansion [18] of the displacement components, is given by,

$$u(x,z,t) = u_0(x,t) + z\theta_x(x,t) + z^2 u_0^*(x,t)$$
$$+ z^3 \theta_x^*(x,t) \tag{1}$$

$$w(x,z,t) = w_0(x,t) + z\theta_z(x,t) + z^2 w_0^*(x,t) \tag{2}$$

where u_0 and w_0 are axial and transverse displacements in the x–z plane at time t, θ_x is the rotation of the cross-section about the y-axis and u_0^*, θ_x^*, θ_z and w_0^* are higher-order terms arising out of the Taylor series expansion and defined at the neutral axis.

The total energy of a system can be given by

$$L = T - \Pi, \tag{3}$$

$$\Pi = U - W_e \tag{4}$$

where U is the internal strain energy, W_e is the work done by the external forces, and T is the kinetic energy.

The strain energy can be expressed as

$$U_s = U_f + U_s \tag{5}$$

where U_f is due to flexure and transverse normal strain and U_s is due to transverse shear strain.

Equation (3) can be rewritten as

$$L = \frac{1}{2} \int \dot{u}' \rho \dot{u} \, dv - \left[\frac{1}{2} \int \varepsilon' \sigma \, dv - \int u' F \, dv \right] \tag{6}$$

where $u = [uw]'$, $\dot{u} = [\dot{u}\dot{w}]'$, $\varepsilon = [\varepsilon_x \varepsilon_z \gamma_{xz}]'$, $\sigma = [\sigma_x \sigma_z \tau_{xz}]'$ and $F = [f_x f_z]'$ and the nodal displacement vector is

$$d = [u_0 w_0 \theta_x u_0^* \theta_x^* \theta_z w_0^*]' \tag{7}$$

The generic displacement vector can be expressed as

$$u = \underline{Z}_d d \tag{8}$$

where

$$\underline{Z}_d = \begin{bmatrix} 1 & 0 & z & z^2 & z^3 & 0 & 0 \\ 0 & 1 & 0 & 0 & 0 & z & z^2 \end{bmatrix} \tag{9}$$

The bending and transverse normal strains are given as

$$\varepsilon_x = \varepsilon_{x0} + z^2 \varepsilon_{x0}^* + zK_x + z^3 K_x^* \tag{10}$$

$$\varepsilon_z = \varepsilon_{z0} + zK_z \tag{11}$$

where

$$[\varepsilon_{x0} \varepsilon_{x0}^* \varepsilon_{z0} K_x K_x^* K_z] = [u_{0,x} u_{0,x}^* \theta_z \theta_{x,x} \theta_{x,x}^* 2w_0^*] \tag{12}$$

and taken together as

$$\varepsilon = [\varepsilon_x \varepsilon_z]' = \underline{Z}\bar{\varepsilon} \tag{13}$$

where

$$\underline{Z} = \begin{bmatrix} 1 & z^2 & 0 & z & z^3 & 0 \\ 0 & 0 & 1 & 0 & 0 & z \end{bmatrix} \tag{14}$$

and

$$\bar{\varepsilon} = [\varepsilon_{x0} \varepsilon_{x0}^* \varepsilon_{z0} K_x K_x^* K_z]' \tag{15}$$

Similarly, the shear strain can be expressed as

$$\gamma_{xz} = \phi + z^2 \phi^* + zK_{xz} \tag{16}$$

where

$$[\phi \phi^* K_{xz}]$$
$$= [(w_{0,x} + \theta_x)(w_{0,x}^* + 3\theta_x^*)(\theta_{z,x} + 2u_0^*)] \tag{17}$$

and can be expressed in the matrix form as

$$\gamma_{xz} = \underline{Z}_{xz}' \bar{\gamma}_{xz} \tag{18}$$

where

$$\underline{Z}_{xz} = [1 z^2 z]' \tag{19}$$

$$\bar{\gamma}_{xz} = [\phi \phi^* K_{xz}]' $$

The stress–strain relationship of an orthotropic lamina in a 3D state of stress can be given as [19]

$$\sigma^* = \underline{Q}^* \varepsilon^* \tag{21}$$

where

$$\sigma^* = [\sigma_x \sigma_y \sigma_z \tau_{xy} \tau_{yz} \tau_{xz}]' \tag{22}$$

$$\varepsilon^* = [\varepsilon_x \varepsilon_y \varepsilon_z \gamma_{xy} \gamma_{yz} \gamma_{xz}]' \tag{23}$$

and $\underline{Q}^*$ is given by eqn (A1) in the Appendix.

By setting σ_y, τ_{xy} and τ_{yz} equal to zero in eqn (21), and deriving σ_x, σ_z and τ_{xz} from that [20] to model the plane stress situation for the 2D beam bending problem, results in the stress–strain relation as,

$$\sigma = \underline{Q}\varepsilon \tag{24}$$

where

$$\sigma = [\sigma_x \sigma_z \tau_{xz}]' \tag{25}$$

$$\varepsilon = [\varepsilon_x \varepsilon_z \gamma_{xz}]' \tag{26}$$

$$\underline{Q} = \begin{bmatrix} & \underline{D} & & 0 \\ & & & 0 \\ 0 & 0 & \underline{D}_{xz} \end{bmatrix} \tag{27}$$

$$\underline{D} = \begin{bmatrix} \bar{Q}_{11} & \bar{Q}_{12} \\ \bar{Q}_{12} & \bar{Q}_{22} \end{bmatrix} \quad \underline{D}_{xz} = [\bar{Q}_{33}] \tag{28}$$

and the expansion of $\underline{D}$ and $\underline{D}_{xz}$ are available in eqns (A2)–(A5).

The internal strain energy due to flexure and transverse normal strain, after carrying out the integration across the cross-section becomes

$$U_f = \frac{1}{2} \int \bar{\varepsilon}' \bar{\sigma} \, dx \tag{29}$$

where

$$\bar{\sigma} = \underline{\bar{D}}\bar{\varepsilon} \tag{30}$$

The stress resultants are given by

$$\bar{\sigma} = [N_x N_x^* N_z M_x M_x^* M_z]' \tag{31}$$

and

$$\underline{\bar{D}} = b \sum_{L=1}^{NL} \int_{h_{L-1}}^{h_L} \underline{Z}' \underline{D} \underline{Z} \, dz \tag{32}$$

which appears in a matrix form as,

$$\underline{\bar{D}} = \begin{bmatrix} \bar{D}_m & \bar{D}_c \\ \bar{D}_c' & \bar{D}_f \end{bmatrix} \tag{33}$$

and $\bar{D}_m$ and $\underline{\bar{D}}_f$ are presented in eqns (A6)–(A8).

Similarly, the internal strain energy due to transverse shear is

$$U_s = \frac{1}{2} \int \bar{\gamma}_{xz}^t \bar{\tau}_{xz} \, dx \tag{34}$$

where

$$\bar{\tau}_{xz} = \underline{D}_{xz} \bar{\gamma}_{xz} \tag{35}$$

The shear stress resultants are given by

$$\bar{\tau}_{xz} = [QQ^*S]^t \tag{36}$$

and

$$\underline{D}_{xz} = b \sum_{L=1}^{NL} \int_{h_{L-1}}^{h_L} \underline{Z}_{xz}^t D_{xz} Z_{xz} \, dz \tag{37}$$

and eqn (A9) gives the expansion of this matrix.

The kinetic energy can be expressed using eqn (8) as

$$T = \frac{1}{2} \int \dot{d}^t \underline{m} \dot{d} \, dx \tag{38}$$

and

$$\underline{m} = b \sum_{L=1}^{NL} \int_{h_{L-1}}^{h_L} \underline{Z}_d^t \rho_L \underline{Z}_d \, dz \tag{39}$$

where ρ_L is the mass density of a particular layer and is presented in eqn (A10).

The external work done is modified using eqn (8) as,

$$W_e = \int d^t \bar{F} \, dx \tag{40}$$

where

$$\bar{F} = \underline{Z}_d^t F \tag{41}$$

$$= [f_{x0}, f_{z0}, m_{x0}, f_{x0}^*, m_{x0}^*, m_{z0}, f_{z0}^*]^t \tag{42}$$

Now, the total energy reappears with eqns (29), (34), (38) and (40) as

$$L = 1/2 \int \dot{d}^t \underline{m} \dot{d} \, dx - \left[1/2 \int \bar{\varepsilon}^t \bar{\sigma} \, dx \right.$$
$$\left. + 1/2 \int \bar{\gamma}_{xz}^t \bar{\tau}_{xz} \, dx - \int d^t \bar{F} \, dx \right] \tag{43}$$

3. Finite-element modelling

In isoparametric formulations, the displacements within an element can be expressed in terms of its nodal displacements as

$$d = \underline{N} a_e \tag{44}$$

where a_e is a vector containing nodal displacement vectors of an element and is given by

$$a_e = [d_1^t d_2^t d_3^t \ldots d_n^t]^t \tag{45}$$

and $\underline{N}$ is the shape function matrix.

Similarly, the flexural and transverse normal strain within an element can be written as

$$\bar{\varepsilon} = \underline{B} a_e \tag{46}$$

and transverse shear strain as

$$\bar{\gamma}_{xz} = \underline{B}_{xz} a_e \tag{47}$$

where $\underline{B}$ and $\underline{B}_{xz}$ are strain displacement matrices.

Table 1
Data table

No.	Description	Ref.
I	*Modelling data*	
	Beam length = 30 in (762 mm)	
	width = 1 in (25.4 mm)	
	$L/D = 5$	
	Load intensity = -300 lb/in (-52.556 N/mm)	
	Number of elements employed = 4 cubic	
II	*Boundary conditions*	
	$u_0 = w_0 = u_0^* = w_0^* = 0$ at $x = 0$ and $x = L$	
III	*Non-dimensionalising factors*	
	$\bar{u}(0,z) = u(0,z)E_z/(-q)$	
	$\bar{\sigma}_x(L/2,z) = \sigma_x(L/2,z)b/(-q)$	
IV	*Data types*	
DATA-1	Face properties:	[23]
	Material: graphite/epoxy	
	t_f (top/bot) = 0.6 in (15.24 mm)	
	$E_x = 0.1742E8$ psi (0.12E6 N/mm^2)	
	$E_y = E_z = 0.1147E7$ psi (0.79E4 N/mm^2)	
	$G_{xy} = 0.7983E6$ psi (0.55E4 N/mm^2)	
	$G_{xy} = G_{yz} = G_{xz}$	
	$\rho = 0.1433E-3$ lb-sec^2/in^4 (1.58 kN-sec^2/m^4)	
	$v = 0.3$	
	Core properties:	[24]
	Material: US commercial aluminium, honey-comb 0.25 in cell size, 0.007 in foil.	
	$t_c = 4.8$ in (121.92 mm)	
	$G_{yz} = 0.1021E5$ psi (70.35 N/mm^2)	
	$G_{xz} = 0.2042E5$ psi (140.7 N/mm^2)	
	$\rho = 0.3098E-5$ lb-sec^2/in^4 (34.15 N-sec^2/m^4)	
	$t_c/t_f = 8$	
	No. of layers of c/s = 10	
	Lamination scheme: 0/30/45/60/core/60/45/30/0	
DATA-2	Lamination scheme: 0/90/core/0/90	
	Rest are same as DATA-1.	
DATA-3	$t_1 = 1$ in (25.4 mm)	[25]
	$E_x = 0.762E8$ psi (0.525E6 N/mm^2)	
	$E_y = E_z = 0.3048E7$ psi (0.21E5 N/mm^2)	
	$G_{xy} = 0.1524E7$ psi (0.105E5 N/mm^2)	
	$G_{xy} = G_{yz} = G_{xz}$	
	$\rho = 0.72567E-4$ lb-sec^2/in^4 (800 N-sec^2/m^4)	
	$v = 0.25$	
	No. of layers of c/s = 6	
	Lamination scheme: 0/90/0	
DATA-4	No. of layers of c/s = 8	
	Lamination scheme: 0/45/−45/90	
	Rest are same as DATA-3.	
V	*Note*	
	HOBT: Higher-order beam theory	
	FOBT: First-order beam theory of Timoshenko	

The non-zero elements of $\underline{B}$ corresponding to a particular node i can be given as

$$B_{11} = B_{24} = B_{43} = B_{55} = N_{i,x}; \quad B_{36} = N_i; \quad B_{67} = 2N_i \quad (48)$$

and of $\underline{B}_{xz}$ as

$$B_{12} = B_{27} = B_{36} = N_{i,x}; \quad B_{13} = N_i; \quad B_{34} = 2N_i; \quad B_{25} = 3N_i \quad (49)$$

With eqns (44), (46) and (47), the total energy can be rewritten as

$$L = 1/2\dot{a}_e^t \int \underline{N}^t \bar{m} \underline{N} \, dx \, \dot{a}_e - \left[1/2 a_e^t \int \underline{B}^t \bar{\sigma} \, dx \right.$$
$$\left. + 1/2 a_e^t \int \underline{B}_{xz}^t \bar{\tau}_{xz} \, dx - a_e^t \int \underline{N}^t \bar{F} \, dx \right] \quad (50)$$

Applying the Hamilton's principle on L, we get the equation of motion as,

$$\underline{M} \ddot{d} + P = f(t) \quad (51)$$

where

$$\underline{M} = \int \underline{N}^t \bar{m} \underline{N} \, dx \quad (52)$$

$$P = \int \underline{B}^t \bar{\sigma} \, dx + \int \underline{B}_{xz}^t \bar{\tau}_{xz} \, dx \quad (53)$$

$$f(t) = \int \underline{N}^t \bar{F} \, dx \quad (54)$$
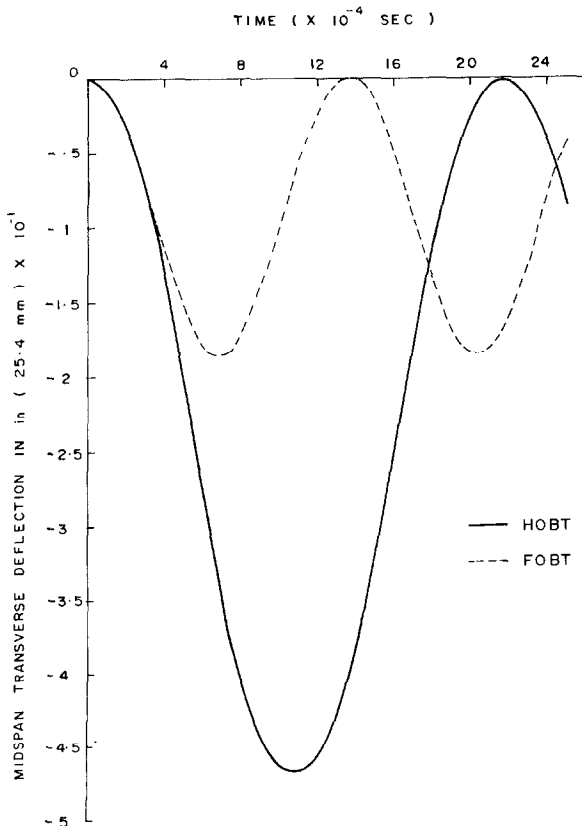
Fig. 1. Midspan transverse deflection of symmetric sandwich beam (Data-1).
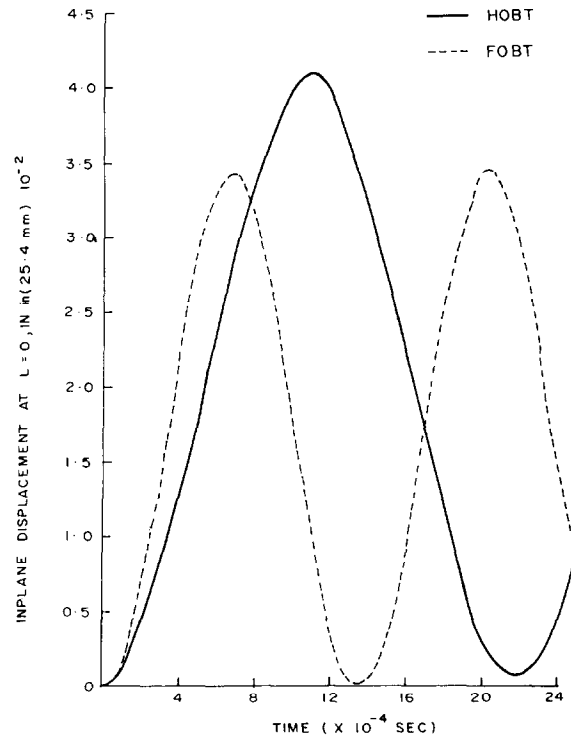
Fig. 2. In-plane displacement of symmetric sandwich beam (Data-1).
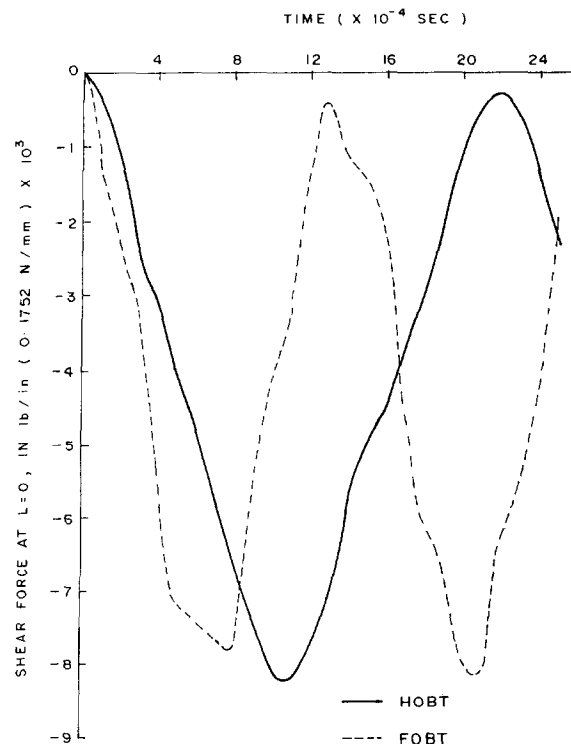
Fig. 3. Shear force variation of symmetric sandwich beam (Data-1).

The consistent mass matrix is evaluated as,

$$\underline{M}_e = \sum_{g=1}^{LG} W_g \underline{N}^t \bar{m} \underline{N} |J| \qquad (55)$$

where LG is the (Total) Number of Gauss Points (four in this case), W_g is the weighing coefficient and $|J|$ is the determinant of Jacobian.

If the total mass of an element can be given by,

$$m_t = \int \rho \, dv \qquad (56)$$

and the sum of diagonal coefficients, corresponding to any translational degree of freedom, of the consistent mass matrix given by eqn (55), is termed as Σm_{tr}, then the specially lumped mass matrix can be obtained [21] by scaling all the diagonal elements of the consistent mass matrix as

$$\bar{m}_{ii} = \bar{m}_{ii}.m_t/\Sigma m_{tr} \qquad (57)$$

and making all the off-diagonal terms of the consistent mass matrix as zero.

The internal resisting force vector can be evaluated as

$$P = \sum_{g=1}^{NG} W_g \underline{B}^t \bar{\sigma} |J| + \sum_{g=1}^{MG} W_g \underline{B}_{xz}^t \bar{\tau}_{xz} |J| \qquad (58)$$

where NG is four for bending and MG is three for shear term evaluation.
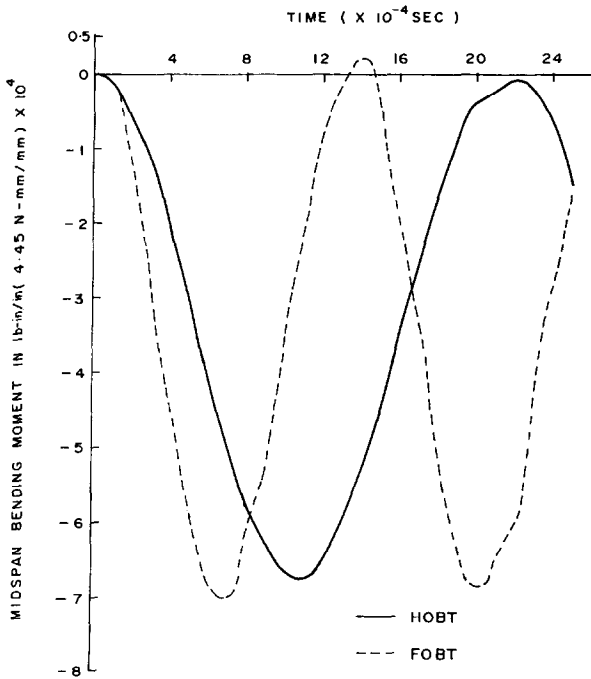
Fig. 4. Bending moment variation of symmetric sandwich beam (Data-1).
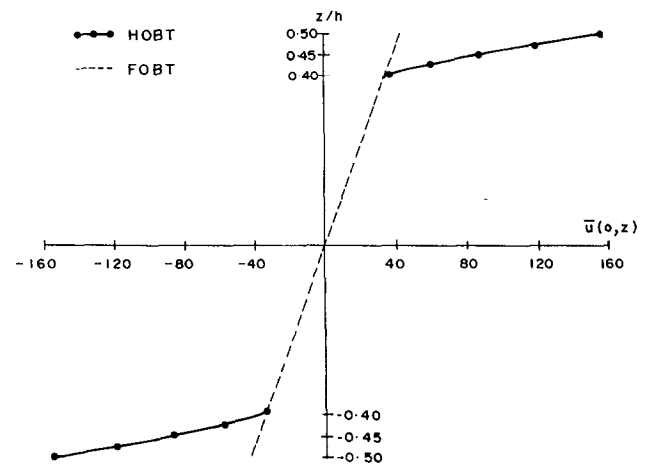
Fig. 5. In-plane displacement distribution of symmetric sandwich beam at $t = 0.11E - 2$ sec (Data-1).
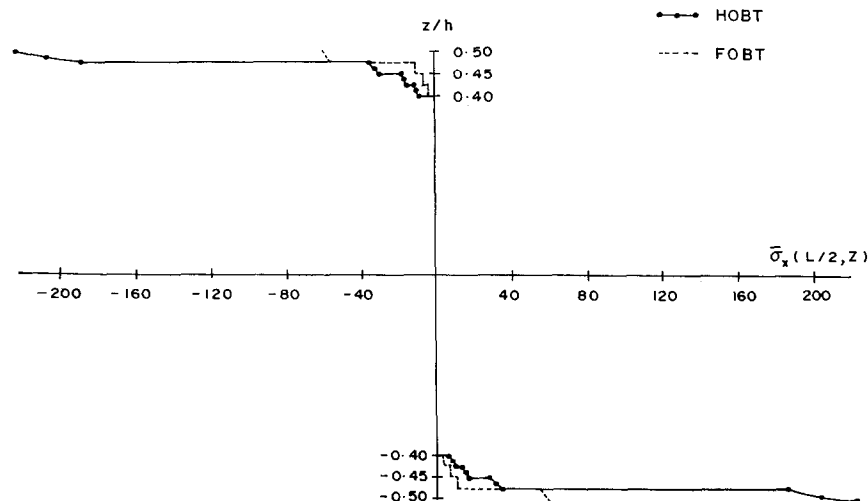
Fig. 6. In-plane stress distribution of symmetric sandwich beam at $t = 0.11E - 2$ sec (Data-1).
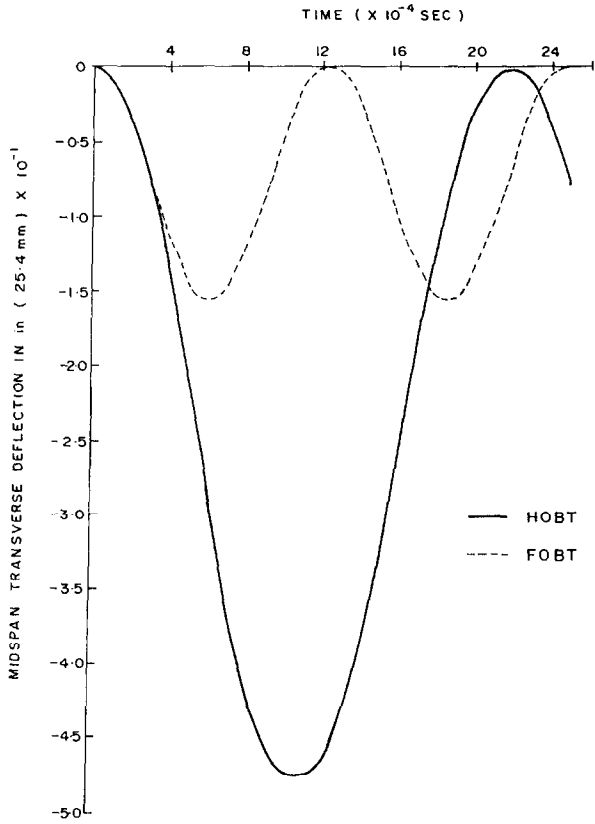
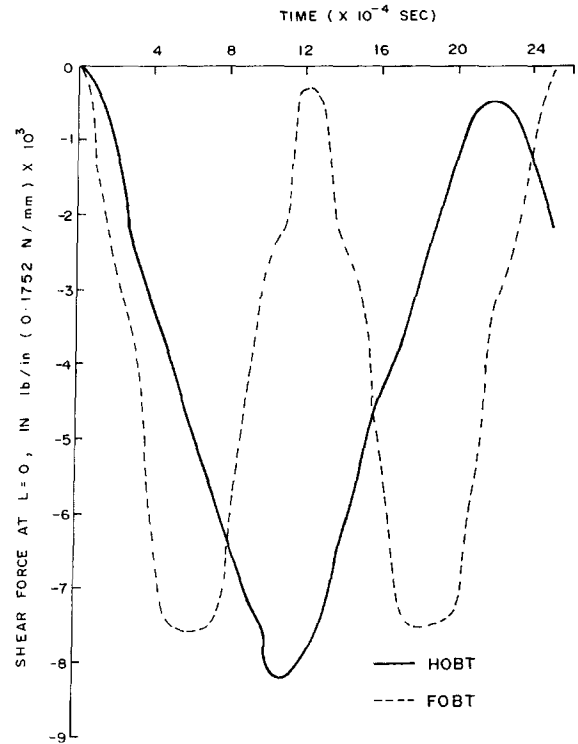Fig. 7. Midspan transverse deflection of unsymmetric sandwich beam (Data-2).

Fig. 9. Shear force variation of unsymmetric sandwich beam (Data-2).
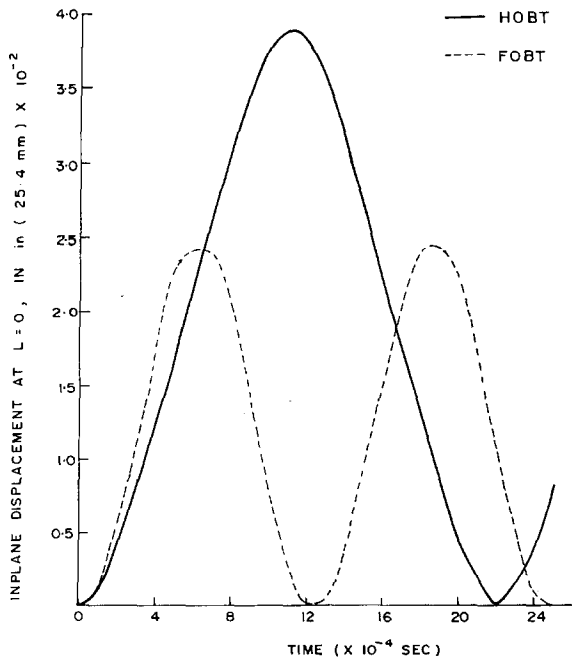

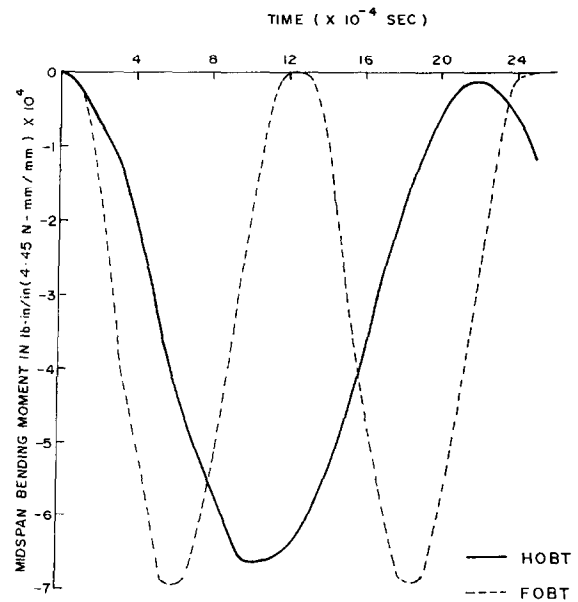Fig. 8. In-plane displacement of unsymmetric sandwich beam (Data-2).

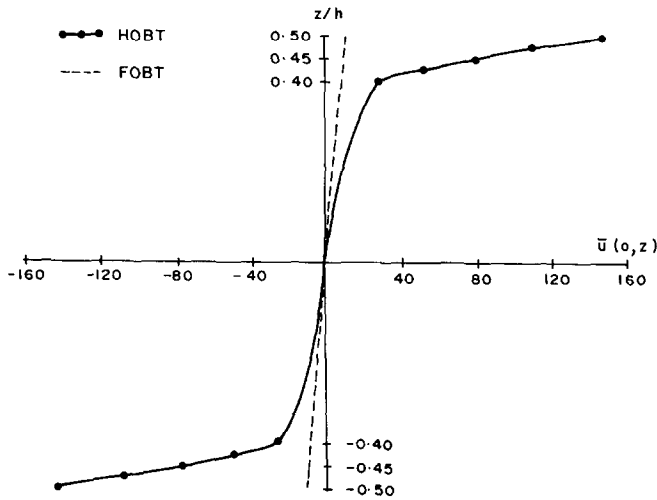Fig. 10. Bending moment variation of unsymmetric sandwich beam (Data-2).

Fig. 11. In-plane displacement distribution of unsymmetric sandwich beam at $t = 0.11E - 2$ sec (Data-2).

The consistent load vector due to a uniformly distributed transverse load q at the top surface of the beam is given by

$$f(t) = \sum_{g=1}^{KG} W_g \underline{N}^t \bar{F} |J| \qquad (59)$$

where

$$\bar{F} = [0, q, 0, 0, 0, qh/2, qh^2/4] \qquad (60)$$

and KG is three.

The governing equation of motion is solved using the central difference predictor technique [22] to obtain the response history at different time steps.

4. Numerical experiments

In order to test the proposed higher-order model, beams with both sandwich and composite constructions subjected to transverse dynamic loadings are considered in this study. Isoparametric cubic elements are employed to discretize the beam. All the experi-
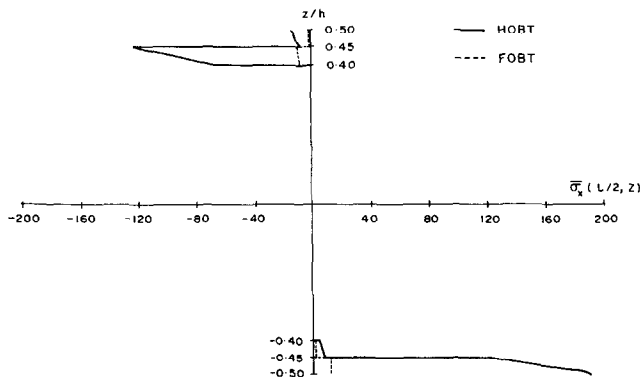

Fig. 12. In-plane stress distribution of unsymmetric sandwich beam at $t = 0.11E - 2$ sec (Data-2).
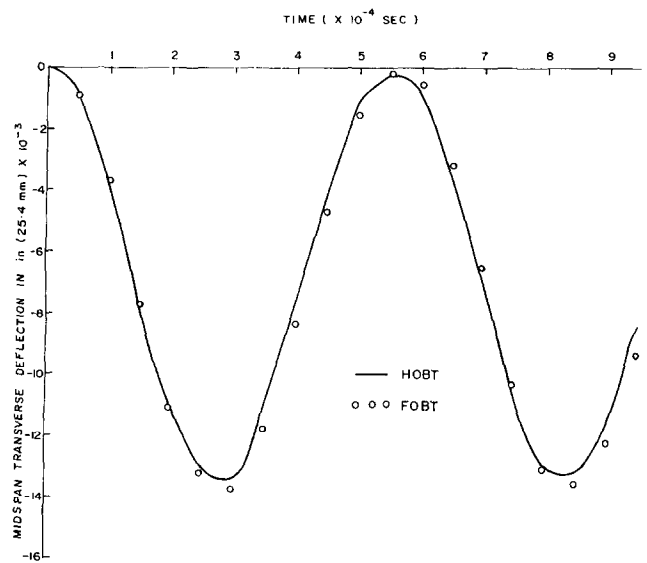

Fig. 13. Midspan transverse deflection of symmetric composite beam (Data-3).

ments are carried out on a pentium machine with DOS in double precision.

4.2. Sandwich beams

A symmetric sandwich beam with properties as described in DATA-1 (Table 1) is considered first. The higher-order transverse displacement is almost three
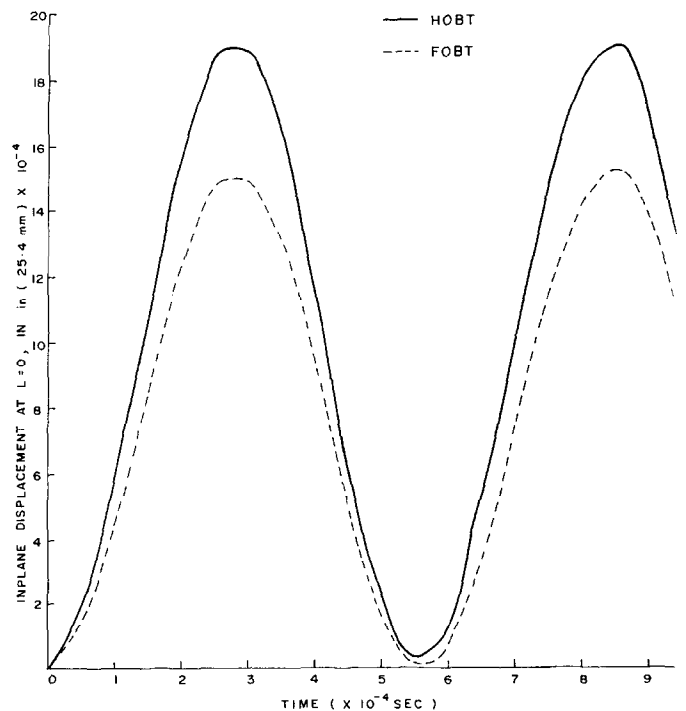

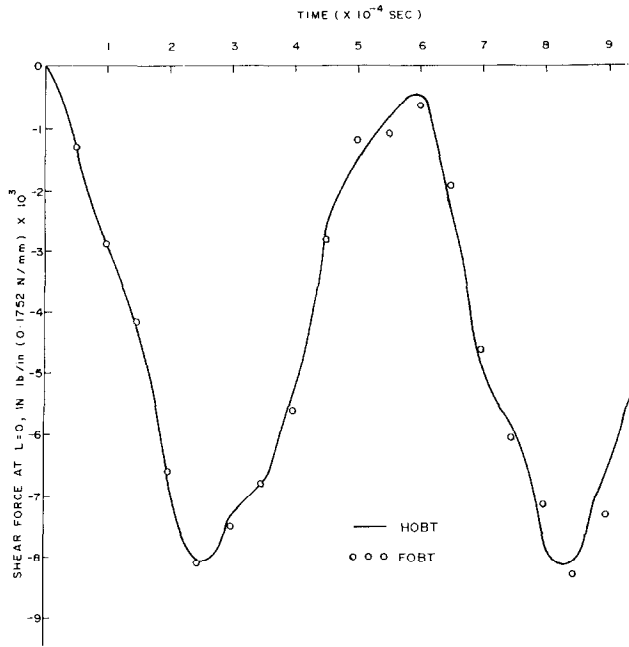Fig. 14. In-plane displacement of symmetric composite beam (Data-3).

Fig. 15. Shear force variation of symmetric composite beam (Data-3).

Fig. 17. In-plane displacement distribution of symmetric composite beam at $t = 0.3E - 3$ sec (Data-3).

Next, an unsymmetric sandwich beam is considered (DATA-2). The higher-order transverse and in-plane displacements are 3 and 1.6 times, respectively, higher than those of the Timoshenko theory (Figs 7 and 8).

times greater and the in-plane displacement is 1.2 times more than those of the first-order theory (Figs 1 and 2). While the amplitude of the higher-order shear force is marginally higher, the higher-order bending moment is marginally lower than that of the Timoshenko theory (Figs 3 and 4). However, in both cases, the higher-order period is nearly 70% more than the first-order period. The in-plane displacement and stress distribution of the higher-order theory clearly brings out the non-linear variation across the depth as shown in Figs 5 and 6.
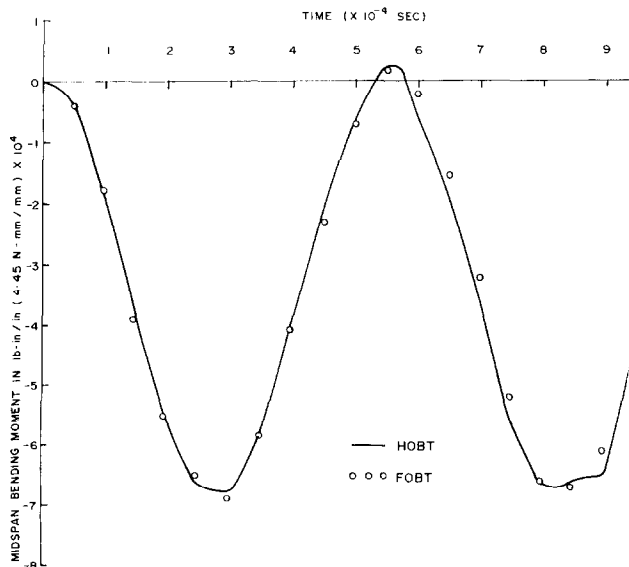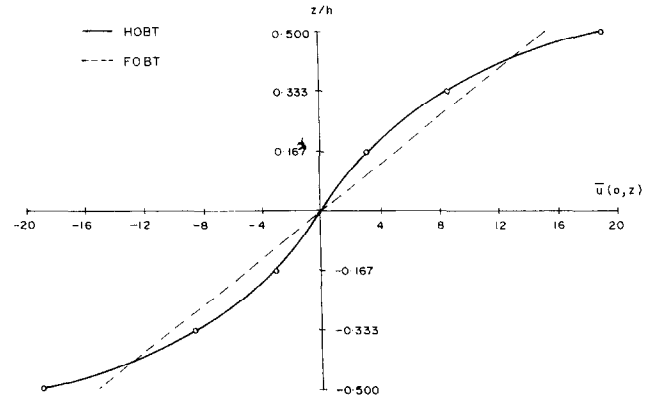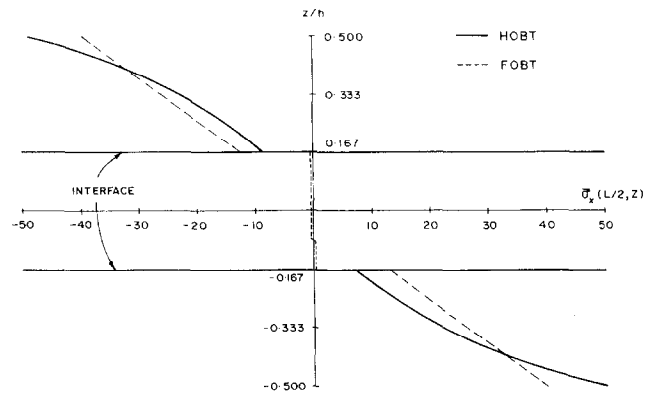

Fig. 18. In-plane stress distribution of symmetric composite beam at $t = 0.3E - 3$ sec (Data-3).

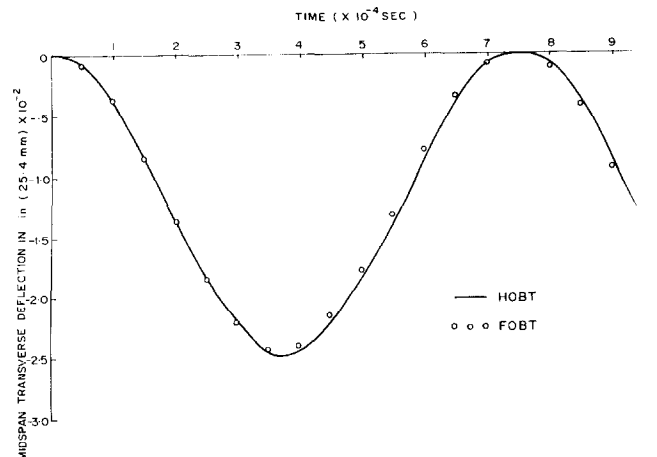Fig. 16. Bending moment variation of symmetric composite beam (Data-3).

Fig. 19. Midspan transverse deflection of unsymmetric composite beam (Data-4).
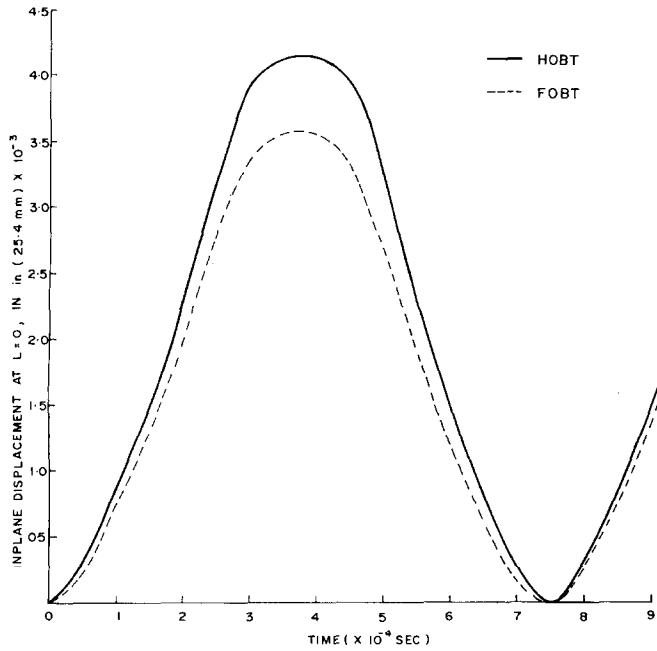
Fig. 20. In-plane displacement of unsymmetric composite beam (Data-4).

The period of the higher-order shear force and bending moment is 83% more than their first-order counterparts (Figs 9 and 10). The non-linear nature of the in-plane displacement and stress distribution of the higher-order theory can be observed in Figs 11 and 12.

4.2. Composite beams

In the case of the symmetric composite beam (DATA-3), the transverse displacement, shear force and bending moment (Figs 13, 15 and 16) by both
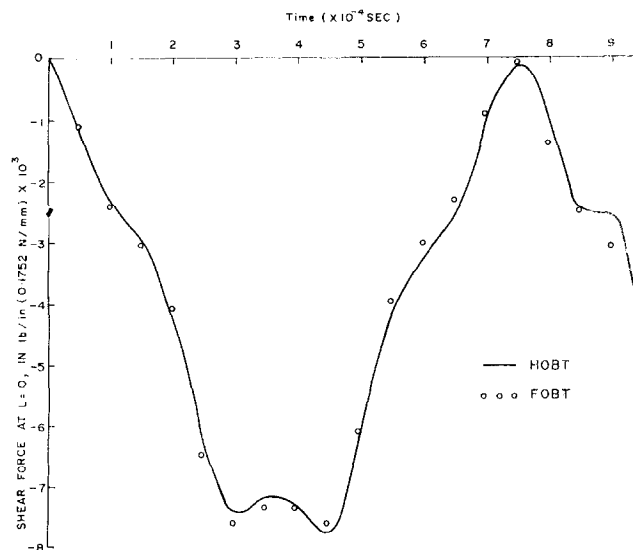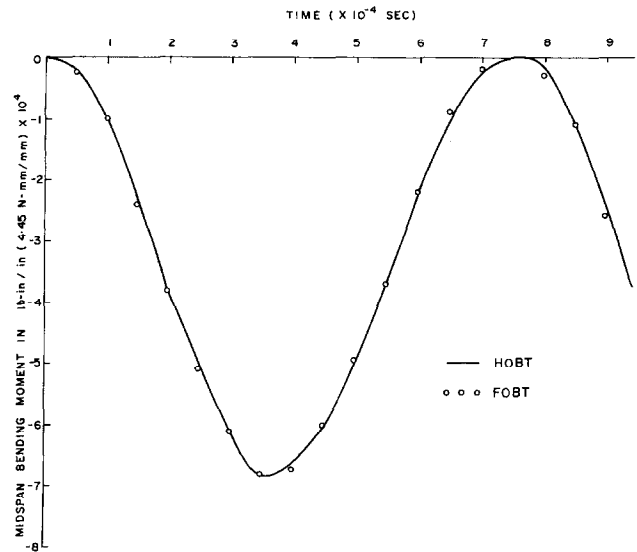

Fig. 22. Bending moment variation of unsymmetric composite beam (Data-4).

theories are very close. The higher-order in-plane displacement is 1.26 times higher than that of the first-order theory (Fig. 14). The non-linear variation of the higher-order in-plane displacement and stress and the linear variation of the Timoshenko theory are depicted in Figs 17 and 18.

In the case of the unsymmetric composite beam (DATA-4) also, the transverse displacement, shear force and bending moment (Figs 19, 21 and 22) by both theories are quite close and the higher-order in-plane displacement is 15% higher than the first-order predictions (Fig. 20). While the in-plane displacement across the depth by the higher-order model is non-linear (Fig. 23), the in-plane stresses by both theories are very close (Fig. 24).

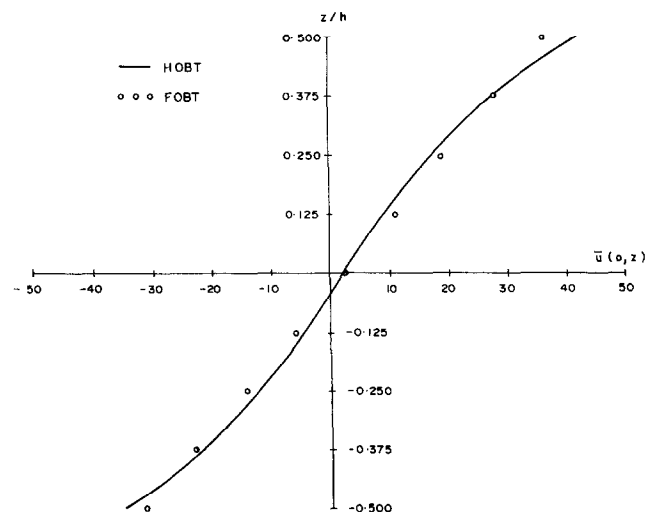Fig. 21. Shear force variation of unsymmetric composite beam (Data-4).

Fig. 23. In-plane displacement distribution of unsymmetric composite beam at $t = 0.35E - 3$ sec (Data-4).
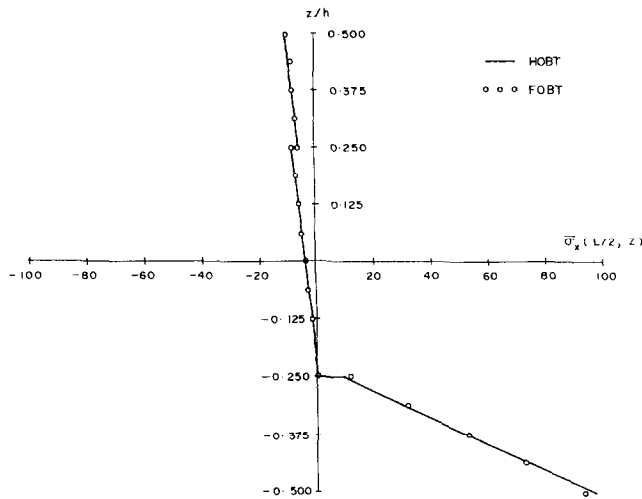
Fig. 24. In-plane stress distribution of unsymmetric composite beam at $t = 0.35E - 3$ sec (Data-4).

5. Conclusions

A higher-order model, which incorporates both the transverse shear and transverse normal strain, for the transient dynamics of laminated beams is presented in this paper. With the adaptation of a constitutive relationship, reduced from the 3D stress–strain relation of an orthotropic lamina, even cross-ply laminates could be analysed using the 2D beam formulation itself. It can be observed from the experiments that the higher-order model is quite effective for the analysis of sandwich constructions. In the case of composites, though global responses of the beam are identically predicted by both these theories, the in-plane displacement and stress distribution across the depth by the higher-order model clearly brings out their non-linear variation, establishing its superior computational potency over the first-order theory.

References

[1] Popov EP. Introduction to Mechanics of Solids. New Delhi: Prentice-Hall of India Pvt. Ltd, 1973.

[2] Paz M. Structural Dynamics — Theory and Computation. Van New Jersey: Nostrand Reinhold, USA, 1985.

[3] Toridis TG, Khozeimeh K. Inelastic response of frames to dynamic loads. ASCE J Engng Mech Div 1971;97:847–863.

[4] Wu RWH, Witmer EA. Finite-element analysis of large elastic–plastic transient deformations of simple structures. AIAA J 1971;9:1719–1724.

[5] Timoshenko SP. On the correction for shear of differential equation for transverse vibrations of prismatic bars. Philos. Mag Series 1921;41:744–746.

[6] Archer J. Consistent matrix formulations for structural analysis using finite element techniques. AIAA J 1965;3:1910–1928.

[7] Kapur K. Vibrations of a Timoshenko beam using finite element approach. J Acoust Soc America 1966;40:1058–1063.

[8] Davis R, Henshell RD, Warburton GB. A Timoshenko beam element. J Sound Vib 1972;22:475–487.

[9] Nickel R, Secor G. Convergence of consistently derived Timoshenko beam finite elements. Int J Numer Meth Engng 1972;5:243–253.

[10] Hughes TJR, Taylor RL, Kanoknukulchai S. A simple and efficient finite element for bending. Int. J. Numer. Meth. Engng. 1977;11:1529–1543.

[11] Kant T, Marur S. R. A comparative study of C^0 and C^1 elements for linear and nonlinear transient dynamics of building frames. Comput Struct 1991;40:659–678.

[12] Stephen NG, Levinson M. A second order beam theory. J Sound Vib 1979;67:293–305.

[13] Heyliger PR, Reddy JN. A higher order beam finite element for bending and vibration problems. J Sound Vib 1988;126:309–326.

[14] Levinson M. A new rectangular beam theory. J. Sound Vib. 1981;74:81–87.

[15] Kant T, Gupta A. A finite element model for a higher-order shear-deformable beam theory. J Sound Vib 1988;125:193–202.

[16] Marur SR, Kant T. Free vibration analysis of fiber reinforced composite beams using higher order theories and finite element modelling. J Sound Vib 1996;194:337–351.

[17] Marur SR, Kant T. On the performance of higher order theories for transient dynamic analysis of sandwich and composite beams. Comput Struct 1997;65:741–759.

[18] Lo KH, Christensen RM, Wu EM. A higher order theory of plate deformation — Part 1: Homogeneous plates. ASME J. Appl Mech. 1977;44:663–668.

[19] Jones RM. Mechanics of Composite Materials. Tokyo: McGraw-Hill, Kogakusha Ltd, 1975.

[20] Vinayak RU, Prathap G, Naganarayana BP. Beam elements based on a higher order theory — I. Formulation and analysis of performance. Comput Struct 1996;58:775–789.

[21] Hinton E, Rock T, Zienkiewicz OC. A note on mass lumping and related processes in the finite element method. Int J Earthq Engng Struct Dyn 1976;4:245–249.

[22] Marur SR, Kant T. A modified form of the central difference predictor scheme for damped nonlinear systems. Comput Struct 1994;50:615–618.

[23] Chen JK, Sun CT. Nonlinear transient responses of initially stressed composite plates. Comput Struct 1985;21:513–520.

[24] Allen HG. Analysis and Design of Structural Sandwich Panels. London: Pergamon Press, 1969.

[25] Reddy JN. On the solutions to forced motions of rectangular composite plates. ASME J Appl Mech 1982;49:403–408.

Appendix

$$Q^* = \begin{bmatrix} Q_{11}^* & Q_{12}^* & Q_{13}^* & Q_{14}^* & 0 & 0 \\ Q_{21}^* & Q_{22}^* & Q_{23}^* & Q_{24}^* & 0 & 0 \\ Q_{31}^* & Q_{32}^* & Q_{33}^* & Q_{34}^* & 0 & 0 \\ Q_{41}^* & Q_{42}^* & Q_{43}^* & Q_{44}^* & 0 & 0 \\ 0 & 0 & 0 & 0 & Q_{55}^* & Q_{56}^* \\ 0 & 0 & 0 & 0 & Q_{65}^* & Q_{66}^* \end{bmatrix}$$

(A1)

$$\bar{Q}_{11} = Q_{11}^* + Q_{12}^*(Q_{14}^*Q_{24}^* - Q_{12}^*Q_{44}^*)/(Q_{22}^*Q_{44}^* - Q_{24}^*Q_{24}^*) + Q_{14}^*(Q_{12}^*Q_{24}^* - Q_{14}^*Q_{22}^*)/(Q_{22}^*Q_{44}^* - Q_{24}^*Q_{24}^*) \tag{A2}$$

$$\bar{Q}_{12} = Q_{13}^* + Q_{12}^*(Q_{24}^*Q_{34}^* - Q_{23}^*Q_{44}^*)/(Q_{22}^*Q_{44}^* - Q_{24}^*Q_{24}^*) + Q_{14}^*(Q_{23}^*Q_{24}^* - Q_{22}^*Q_{34}^*)/(Q_{22}^*Q_{44}^* - Q_{24}^*Q_{24}^*) \tag{A3}$$

$$\bar{Q}_{22} = Q_{33}^* + Q_{23}^*(Q_{24}^*Q_{34}^* - Q_{23}^*Q_{44}^*)/(Q_{22}^*Q_{44}^* - Q_{24}^*Q_{24}^*) + Q_{34}^*(Q_{23}^*Q_{24}^* - Q_{22}^*Q_{34}^*)/(Q_{22}^*Q_{44}^* - Q_{24}^*Q_{24}^*) \tag{A4}$$

$$\bar{Q}_{33} = Q_{66}^* - (Q_{56}^*Q_{56}^*/Q_{55}^*) \tag{A5}$$

$$\underline{\bar{D}}_m = b \sum_{L=1}^{NL} \begin{bmatrix} \bar{Q}_{11}H_1 & \bar{Q}_{11}H_3 & \bar{Q}_{12}H_1 \\ & \bar{Q}_{11}H_5 & \bar{Q}_{12}H_3 \\ & & \bar{Q}_{22}H_1 \end{bmatrix} \tag{A6}$$

$$\underline{\bar{D}}_c = b \sum_{L=1}^{NL} \begin{bmatrix} \bar{Q}_{11}H_2 & \bar{Q}_{11}H_4 & \bar{Q}_{12}H_2 \\ & \bar{Q}_{11}H_6 & \bar{Q}_{12}H_4 \\ & & \bar{Q}_{22}H_2 \end{bmatrix} \tag{A7}$$

$$\underline{\bar{D}}_f = b \sum_{L=1}^{NL} \begin{bmatrix} \bar{Q}_{11}H_3 & \bar{Q}_{11}H_5 & \bar{Q}_{12}H_3 \\ & \bar{Q}_{11}H_7 & \bar{Q}_{12}H_5 \\ & & \bar{Q}_{22}H_3 \end{bmatrix} \tag{A8}$$

$$\underline{\bar{D}}_{xz} = b \sum_{L=1}^{NL} \begin{bmatrix} \bar{Q}_{33}H_1 & \bar{Q}_{33}H_3 & \bar{Q}_{33}H_2 \\ & \bar{Q}_{33}H_5 & \bar{Q}_{33}H_4 \\ & & \bar{Q}_{33}H_3 \end{bmatrix} \tag{A9}$$

$$\underline{\bar{m}} = b \sum_{L=1}^{NL} \rho_L \begin{bmatrix} H_1 & 0 & H_2 & H_3 & H_4 & 0 & 0 \\ & H_1 & 0 & 0 & 0 & H_2 & H_3 \\ & & H_3 & H_4 & H_5 & 0 & 0 \\ & & & H_5 & H_6 & 0 & 0 \\ Sym. & & & & H_7 & 0 & 0 \\ & & & & & H_3 & H_4 \\ & & & & & & H_5 \end{bmatrix} \tag{A10}$$

where

$$H_k = (h_L^k - h_{L-1}^k)/k, k = 1 \dots 7,$$

and *NL* stands for the (Total) Number of Layers of the cross-section.